

# Terahertz two-photon quantum well infrared photodetector

H. Schneider,<sup>1</sup> H. C. Liu,<sup>2</sup> S. Winnerl,<sup>1</sup> C. Y. Song,<sup>2</sup> M. Walther,<sup>3</sup> and M. Helm<sup>1</sup>

<sup>1</sup> Forschungszentrum Dresden Rossendorf, Institute of Ion Beam Physics and Materials Research, P. O. Box 510119, D-01314 Dresden, Germany

<sup>2</sup> Institute for Microstructural Sciences, National Research Council, Ottawa K1A 0R6, Canada

<sup>3</sup> Fraunhofer Institute for Applied Solid State Physics, Tullastr. 72, D-79108 Freiburg, Germany

[h.schneider@fzd.de](mailto:h.schneider@fzd.de)

**Abstract:** A two-photon detector based on intersubband transitions in GaAs/AlGaAs quantum wells operating in the Terahertz regime below the Reststrahlenband is reported. Resonantly enhanced optical nonlinearities enables sensitive quadratic detection at pJ pulse energies. We demonstrate its use in a quadratic autocorrelator for far-infrared picosecond pulses at around 7 THz.

© 2009 Optical Society of America

**OCIS codes:** (040.2235) Detectors, far infrared or terahertz; (190.5970) Semiconductor nonlinear optics including MQW; (300.6530) Spectroscopy, ultrafast.

---

## References and links

1. H. Schneider and H. C. Liu, *Quantum Well Infrared Photodetectors: Physics and Applications* (Springer, 2006).
2. S. D. Gunapala and S. V. Bandara, "Quantum Well Infrared Photodetector Focal Plane Arrays," in *Intersubband Transition in Quantum Wells: Physics and Device Applications I*, Academic Press, San Diego, Semiconductors and Semimetals Vol. 62 2000, ch. 4, pp. 197–282, edited by H. C. Liu and F. Capasso.
3. J. Faist, F. Capasso, D. L. Sivco, C. Sirtori, A. L. Hutchinson, and A. Y. Cho, "Quantum Cascade Laser," *Science* **264**, 553–556 (1994).
4. C. Sirtori and R. Teissier, "Quantum Cascade Lasers: Overview of Basic Principles and State of the Art," in *Intersubband Transitions in Quantum Structures*, R. Paiella, ed. (McGraw-Hill, 2006), pp. 1–44.
5. E. L. Dereniak and G. D. Boreman, *Infrared Detectors and Systems* (Wiley, New York, 1996).
6. D. Weidmann, F. K. Tittel, T. Aellen, M. Beck, D. Hofstetter, J. Faist, and S. Blaser, "Mid-infrared trace-gas sensing with a quasi-continuous-wave Peltier-cooled distributed feedback quantum cascade laser," *Appl. Phys. B* **79**, 907–913 (2004).
7. M. T. McCulloch, N. Langford, and G. Duxbury, "Real-time trace-level detection of carbon dioxide and ethylene in car exhaust gases," *Appl. Opt.* **44**, 2887–2894 (2005).
8. F. Capasso, R. Paiella, R. Martini, R. Colombelli, C. Gmachl, T. L. Myers, M. S. Taubman, R. M. Williams, C. G. Bethea, K. Unterrainer, H. Y. Hwang, D. L. Sivco, A. Y. Cho, M. A. Sergent, H. C. Liu, and E. A. Whittaker, "Quantum cascade lasers: Ultrahigh-speed operation, optical wireless communication, narrow linewidth, and far-infrared emission," *IEEE J. Quantum Electron.* **38**, 511–532 (2002).
9. E. Rosencher, A. Fiore, B. Vinter, V. Berger, Ph. Bois, J. Nagle, "Quantum Engineering of Optical Nonlinearities," *Science* **271**, 168–173 (1996).
10. C. Gmachl, O. Malis, and A. Belyanin, "Optical Nonlinearities in Intersubband transitions and Quantum Cascade Lasers," in *Intersubband Transitions in Quantum Structures*, R. Paiella, ed. (McGraw-Hill, 2006), pp. 181–235.
11. S. S. Dhillon, C. Sirtori, J. Alton, S. Barbieri, A. de Rossi, H. E. Beere, and D. A. Ritchie, "Terahertz transfer onto a telecom optical carrier," *Nat. Photon.* **1**, 411–415 (2007).
12. H. Schneider, T. Maier, H. C. Liu, M. Walther, and P. Koidl, "Ultra-sensitive femtosecond two-photon detector with resonantly enhanced nonlinear absorption," *Opt. Lett.* **30**, 287–289 (2005).
13. H. Schneider, O. Drachenko, S. Winnerl, M. Helm, and M. Walther, "Quadratic autocorrelation of free-electron laser radiation and photocurrent saturation in two-photon quantum-well infrared photodetectors," *Appl. Phys. Lett.* **89**, 133508 (2006).

14. R. Paiella, F. Capasso, C. Gmachl, D. L. Sivco, J. N. Baillargeon, A. L. Hutchinson, A. Y. Cho, H. C. Liu, "Self-Mode-Locking of Quantum Cascade Lasers with Ultrafast Optical Nonlinearities," *Science* **290**, 1739-1742 (2000).
15. A. Gordon, C. Y. Wang, L. Diehl, F. X. Krtner, A. Belyanin, D. Bour, S. Corzine, G. Hfler, H. C. Liu, H. Schneider, T. Maier, M. Troccoli, J. Faist, and F. Capasso, "Multimode regimes in quantum cascade lasers: From coherent instabilities to spatial hole burning," *Phys. Rev. A* **77**, 053804 (2008).
16. C. Y. Wang, L. Kuznetsova, V. M. Gkortsas, L. Diehl, F. Kärtner, M. A. Belkin, A. Belyanin, X. Li, D. Ham, H. Schneider, P. Grant, C. Y. Song, S. Haffouz, Z. R. Wasilewski, H. C. Liu, and F. Capasso, "Stable mode-locked pulses from mid-infrared semiconductor lasers," arXiv:0903.4385v1.
17. H. Schneider, T. Maier, M. Walther, and H. C. Liu, "Two-photon photocurrent spectroscopy of electron intersubband relaxation and dephasing in quantum wells," *Appl. Phys. Lett.* **91**, 191116 (2007).
18. H. Schneider, T. Maier, H. C. Liu, and M. Walther, "Two-photon photocurrent autocorrelation under nearly-resonant excitation," *Opt. Express* **16**, 1523-1528 (2008).
19. R. Köhler, A. Tredicucci, F. Beltram, H. E. Beere, E. H. Linfield, A. G. Davies, D. A. Richie, R. C. Iotti, and F. Rossi, "Terahertz semiconductor-heterostructure laser," *Nature* **417**, 156-159 (2002).
20. B. S. Williams, "Terahertz quantum-cascade lasers," *Nat. Photon.* **1**, 517-525 (2007).
21. H. C. Liu, C. Y. Song, A. J. SpringThorpe, and J. C. Cao, "Terahertz quantum-well photodetector," *Appl. Phys. Lett.* **84**, 4068-4070 (2004).
22. H. Luo, H. C. Liu, C. Y. Song, and Z. R. Wasilewski, "Background-limited terahertz quantum-well photodetector," *Appl. Phys. Lett.* **86**, 231103 (2005).
23. *For a recent review see M. Tonouchi, "Cutting-edge terahertz technology," Nat. Photon.* **1**, 97 (2007).
24. T. Maier, H. Schneider, M. Walther, P. Koidl, and H. C. Liu, "Resonant two-photon photoemission in quantum well infrared photodetectors," *Appl. Phys. Lett.* **84**, 5162-5164 (2004).
25. C. Patel, T. J. Parker, H. Jamshidi, and W. F. Sherman, "Phonon frequencies in GaAs," *Phys. Status Solidi B* **122**, 461-467 (1984).
26. H. C. Liu, C. Y. Song, Z. R. Wasilewski, J. A. Gupta, and M. Buchanan, "Fano resonance mediated by intersubband-phonon coupling," *Appl. Phys. Lett.* **91**, 131121 (2007).
27. H. Schneider, H. C. Liu, S. Winnerl, O. Drachenko, M. Helm, J. Faist, "Room-temperature midinfrared two-photon photodetector," *Appl. Phys. Lett.* **93**, 101114 (2008).
28. S. Ehret, H. Schneider, C. Schönbein, G. Bihlmann, and J. Fleissner, "Analysis of the transport mechanism in GaAs/AlGaAs quantum-well infrared photodetection structures using time resolved photocurrent measurements," *Appl. Phys. Lett.* **69**, 931-933 (1996).

## 1. Introduction

Intersubband transitions in quantum wells (QW) have enabled important devices for mid-infrared optoelectronics, namely quantum well infrared photodetectors (QWIP) [1, 2] and quantum cascade lasers (QCL) [3, 4]. These innovations have formed the basis for emerging applications in thermal imaging, surveillance technology [5], chemical sensing [6, 7], and infrared data transmission [8]. Moreover, intersubband transitions in QWs go along with pronounced optical nonlinearities, resulting in huge nonlinear coefficients for second harmonic generation, more than three orders of magnitude larger than for the host material GaAs [9]. Intersubband transitions have also been exploited for wavelength conversion of QCL radiation [10] and external near-infrared signals [11].

Previously, we have demonstrated quadratic photodetection involving resonant two-photon transitions between three energy levels, namely two bound states  $|1\rangle$ ,  $|2\rangle$ , and one equidistant continuum resonance  $|3\rangle$ . In this configuration, two infrared photons are required to emit an electron into the continuum (Fig. 1(a)), such that the photocurrent scales quadratically with the incident power [12]. This behavior, which contrasts the linear power dependence of standard QWIPs [1], provides the basis for device operation as a quadratic detector. Due to the presence of a real intermediate state, huge optical nonlinearities (six orders of magnitude stronger than GaAs) have been reached, thus resulting in an extremely sensitive nonlinear optical device operating at power densities as low as  $0.1 \text{ Wcm}^{-2}$ . The two-photon QWIP approach has proven useful for quadratic autocorrelation of pulsed mid-infrared sources including frequency-converted radiation from tabletop laser systems [12], free-electron lasers [13], and QCLs. For the latter device, various modes of pulsed operation, including self-pulsations [14], coherent in-

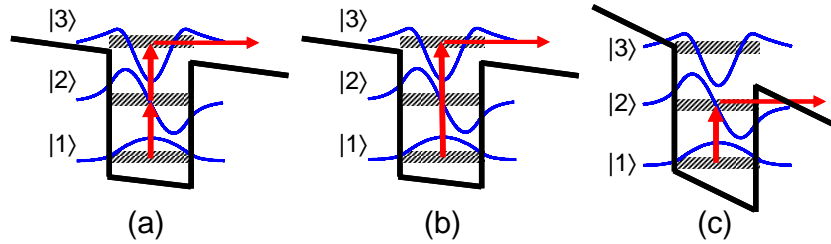


Fig. 1. Band diagrams for (a) quadratic detection associated with transitions  $|1\rangle \rightarrow |2\rangle$  and  $|2\rangle \rightarrow |3\rangle$ , (b) linear detection by transition  $|1\rangle \rightarrow |3\rangle$ , and (c) linear detection involving  $|1\rangle \rightarrow |2\rangle$  assisted by tunneling.

stabilities [15], and modelocking [16] have been demonstrated recently. Besides these applications in mid-infrared pulse diagnostics, the two-photon QWIP also enabled several fundamental investigations of intersubband dynamics [17, 18].

Extending device operation towards far-infrared wavelengths beyond the Reststrahlenband has led to the demonstration of Terahertz (THz)-QCLs [19] and THz-QWIPs [21, 22]. Nonlinear detection in this spectral regime in particular would be promising for applications in THz technology based on femtosecond near-infrared lasers [23] where short THz transients naturally emerge.

In this paper, we demonstrate the first two-photon quantum well infrared photodetector operating in the THz regime beyond the Reststrahlenband. We confirm its quadratic intensity dependence and demonstrate its use in quadratic autocorrelation measurements of far-infrared picosecond pulses from a free-electron laser. Huge optical nonlinearities allow for quadratic detection at THz pulse intensities as low as a few pJ.

## 2. Structural and spectral characteristics

The two-photon THz QWIP under study comprises 20 GaAs QWs of 18 nm width sandwiched between 70 nm wide  $\text{Al}_{0.05}\text{Ga}_{0.95}\text{As}$  barriers. The central 12 nm of each QW are Si-doped to nominally  $1 \times 10^{17} \text{ cm}^{-3}$ , corresponding to a carrier concentration of  $1.2 \times 10^{11} \text{ cm}^{-2}$  per QW. The active region is sandwiched between 400 nm and 700 nm thick n-type GaAs contact layers on the top and substrate sides, respectively. Mesa diodes of  $400 \times 400 \mu\text{m}^2$  and  $600 \times 600 \mu\text{m}^2$  area with metal contacts were fabricated using standard optical lithography and wet-chemical etching. The THz radiation was coupled into the active region via standard 45 degree facets [1].

Figure 2 shows linear photocurrent spectra of the device obtained at low temperature and various bias voltages using a Fourier-transform infrared spectrometer under glowbar illumination. At low bias (0.1 V), the photocurrent sets in at photon energies around  $380 \text{ cm}^{-1}$  due to (linear) excitation from the ground subband into the continuum (see Fig. 1(b)). Note that the transition from  $|1\rangle$  into  $|3\rangle$  is parity forbidden for bound states and symmetric QWs, whereas this parity selection rule is relaxed if state  $|3\rangle$  is located in the continuum. This leads to a gradual photocurrent increase around the cutoff energy. At higher bias (0.5 V), the cutoff exhibits a significantly steeper increase due to the odd parity of the applied electric field and moves to lower energies. No signal is observed at the energy of the  $|1\rangle \rightarrow |2\rangle$  transition since two-photon excitation is negligible at these low intensities.

The situation changes drastically at higher bias (0.94 V and 1.5 V) since carriers excited into subband  $|2\rangle$  gain finite probability to escape from the QW by Fowler-Nordheim tunneling into the continuum (see Fig. 1(c)). This mechanism has been studied previously in more detail [24].

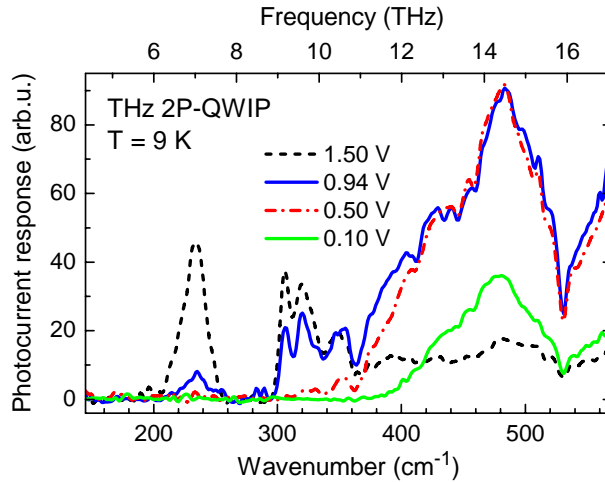


Fig. 2. Linear photocurrent spectra of THz two-photon QWIP at different bias voltages as indicated.

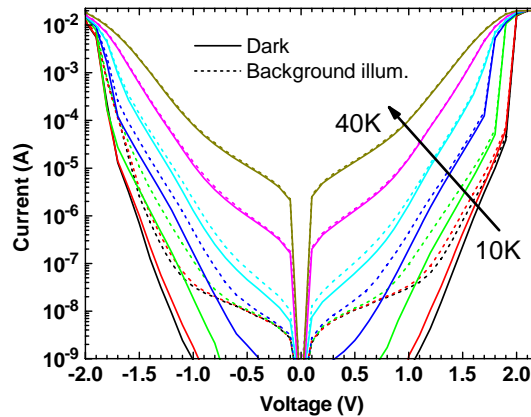


Fig. 3. Current-voltage curves of THz two-photon QWIP at temperatures from 10 K to 40 K in 5 K increments with and without background illumination (56 degrees field-of-view).

We thus observe a pronounced signal peaked at  $235 \text{ cm}^{-1}$  ( $42.5 \mu\text{m}$ ). This is not necessarily the exact peak value for  $|1\rangle \rightarrow |2\rangle$  transition, since it is limited towards higher energies by the Reststrahlenband where no signal is observed due to strong optical-phonon induced absorption in the GaAs substrate. Above  $300 \text{ cm}^{-1}$ , some photoresponse also exists in between the Reststrahlenband and the expected  $|1\rangle \rightarrow |3\rangle$  transition energy. Apparently, the tunnel coupling between the QW and the adjacent continuum becomes efficient enough to generate substantial oscillator strength in this spectral region.

Absorption in the GaAs substrate due to two-phonon transitions at symmetry points of the bandstructure leads to further dips in the spectral shape above the Reststrahlenband. In particular, pronounced features in Fig. 2 at around  $530 \text{ cm}^{-1}$  are caused by two-phonon absorption involving two TO phonons, whereas absorption by LO+TA and TO+TA (2LA and LO+LA) phonons leads to structures in the range  $300\text{-}370 \text{ cm}^{-1}$  ( $400\text{-}460 \text{ cm}^{-1}$ ). These two-phonon

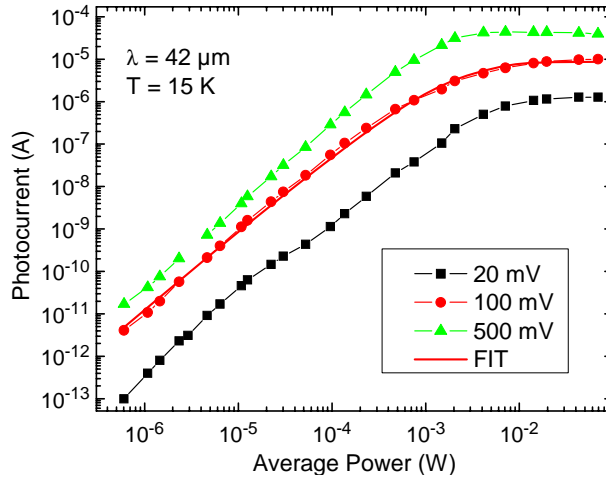


Fig. 4. Measured intensity dependence of the photocurrent at 20 mV, 100 mV, and 500 mV bias, including a fit for 100 mV.

absorption dips are well known from absorption measurements of bulk GaAs (for a detailed assignment of two-phonon absorption lines in GaAs see [25]). This behavior is also typical for THz QWIPs, whereas a Fano lineshape is observed if the active region is involved in the two-phonon transition [26].

Current-voltage curves at varying temperatures are shown in Fig. 3 to investigate the temperature regime for background-limited performance (BLIP). Below 1 V bias, the detector is BLIP up to 25 K. Note that the  $|1\rangle \rightarrow |2\rangle$  transition does not produce any linear signal in this bias regime, such that the cutoff wavelength is given by the  $|1\rangle \rightarrow |3\rangle$  transition (about  $27\ \mu\text{m}$  cutoff wavelength). The observed BLIP temperature is consistent with those of previous THz QWIPs (e. g., 17 K at about  $50\ \mu\text{m}$  cutoff [22]).

### 3. Quadratic detection

For practical quadratic detection experiments, we have used the FELBE free-electron laser facility in Dresden to excite the transition at a wavelength of  $42\ \mu\text{m}$  ( $h\nu = 29.5\ \text{meV}$ ). The two-photon QWIP is operated at a bias of 500 mV and below, such that the tunneling-induced linear photocurrent contribution is sufficiently suppressed. According to Fig. 2, the final state of the two-photon transition ( $2h\nu$ ) fits into the rather broad continuum resonance. Figure 4 shows the photocurrent  $I$  versus the incident power  $P$  of the free-electron laser running quasi-cw at a 13 MHz repetition rate. The observed overall intensity dependence is similar to previous studies on devices with shorter operation wavelength [13, 27]. In particular, the expression [13]

$$I = SP^2W\left(\frac{I_{Sat}}{SP^2}\right), \quad (1)$$

where  $S$  is the prefactor of the quadratic photocurrent,  $I_{Sat}$  the saturation current, and  $W$  Lambert's W-function, yields excellent agreement with the data, as shown in Fig. 4 for 100 mV bias. Expression (1) originates from the approximations that the photoconductive gain depends linearly and the dark current exponentially on the local electric field inside the active region. The little kink at  $20\ \mu\text{W}$  for 20 mV bias is associated with the large dielectric relaxation time [28] at 15 K and low excitation density; it disappears at slightly higher temperatures.

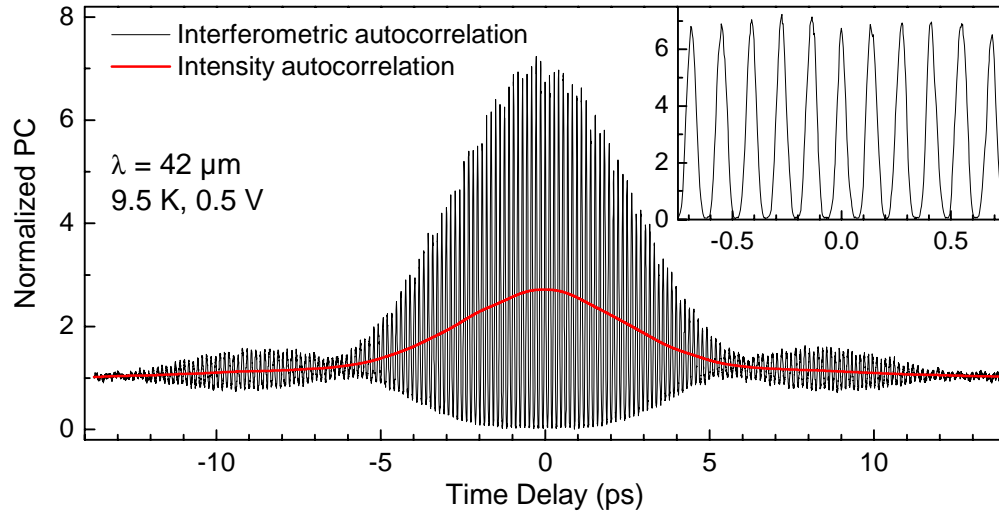


Fig. 5. Interferometric and intensity autocorrelation of FEL pulses at  $42 \mu\text{m}$  (7.1 THz) using a THz two-photon QWIP. Inset: Autocorrelation fringes at an expanded scale.

#### 4. Quadratic autocorrelation of THz pulses

Finally, we apply the THz two-photon QWIP to characterize the time structure of the FEL pulses. For this purpose, a Michelson-interferometer is used to superimpose two pulses at a variable time delay. Here the FEL was strongly attenuated to a total average power of about  $70 \mu\text{W}$  (6 pJ per pulse) which was focused onto the detector. Both interferometric and intensity autocorrelation traces (with the fringes removed by Fourier filtering in the latter) are shown in Fig. 5. The 6.2 ps full-width at half-maximum of the autocorrelation trace indicates an FEL pulse width of 4.4 ps. Nearly perfect quadratic detection becomes evident from the ratio between the signal values at zero delay and at large delay, which amounts to 7.2 (2.7) for interferometric (intensity) autocorrelation, respectively, being close to the theoretical value of 8 (3). The slightly smaller experimental values are attributed to saturation effects [13]. The autocorrelation fringes show a distinctive  $(1-\cos)^2$ -like shape (inset of Fig. 5), which is characteristic for quadratic autocorrelation [13, 27]. The fringing at larger time delay is presumably caused by a delayed pulse replica (by 9 ps), and by residual water vapor absorption. No evidence of detector-limited dynamics could be found, indicating that the intrinsic time constants (intersubband relaxation and dephasing times) are shorter than the investigated signals [12, 18].

#### 5. Conclusion

We have demonstrated a two-photon detector involving intersubband transitions between three energetically equidistant subbands operating in the Terahertz regime beyond the Reststrahlen band. Exploiting the device in a quadratic autocorrelator for far-infrared pulses of a few ps duration at  $42 \mu\text{m}$  (7.1 THz), no limitation induced by intrinsic time constants has been found. Our results demonstrate a new class of ultrafast quadratic autocorrelators with unprecedented sensitivity, suitable for monitoring weak THz pulses of only a few pJ.

#### Acknowledgments

We are grateful to P. Michel (Dresden) and the whole ELBE team for their dedicated support.